Turkish Journal of Science & Technology
17(2), 357-373, 2022

Research Paper
https://doi.org/10.55525/tjst.1113021

Dynamic Response of Concentrically Braced Steel Frames to Pulse Period in Near-Fault Ground Motions

Zeliha TONYALI[1], Muhammet YURDAKUL[2], Hasan SESLİ[3*]

[1] Department of Civil Engineering, The Faculty of Engineering and Architecture, Recep Tayyip Erdoğan University, Rize, Turkey

[2] Department of Civil Engineering, The Faculty of Technology, Karadeniz Technical University, Trabzon, Turkey

[3] Department of Civil Engineering, The Faculty of Engineering, Yalova University, Yalova, Turkey

[1] zeliha.tonyali@erdogan.edu.tr, [2] m.yurdakul@ktu.edu.tr, [*3] hasan.sesli@yalova.edu.tr

(Geliş/Received: 06/05/2022; Kabul/Accepted: 02/08/2022)

Abstract: Steel braced frame systems (SBFs) having high stiffness and high strength are commonly utilized due to their resistance to lateral seismic forces in regions with high seismicity. In this study, concentrically braced frames (CBFs) having different bracing configurations are used to obtain the significance of the pulse period associated with near-fault (NF) ground motion by time-history dynamic analysis. Besides, far-fault (FF) ground motions are also used to compare with NF ground motion results according to chancing bracing configurations. To achieve dynamic responses of steel frames with different concentric bracings under NF ground motions, which especially have small, medium, and long pulse periods, 3-story and 4-span CBFs having different bracing configurations were selected as an example. 4 FF and 12 NF ground motions having different pulse durations were chosen to evaluate the dynamic response of concentrically braced frames. The results showed that peak ground acceleration (PGA) could be identified as a key parameter that controls the response of braced frames under FF ground motions. In addition, the ratio of the pulse duration to the first mode period is the dominant parameter when this ratio is only greater than 1.0 under the NF ground motions.

Key words: Dynamic response, pulse period, near-fault, concentric bracing, steel frames.

Merkezi Çaprazlı Çelik Çerçevelerin Yakın-Fay Yer Hareketlerinin Darbe Periyoduna Dinamik Tepkisi

Öz: Hem yüksek rijitliğe hem de yüksek dayanıma sahip olan çelik çaprazlı çerçeve sistemler, depremselliğin yüksek olduğu bölgelerde yanal sismik yüklere karşı gösterdikleri performans nedeniyle yaygın olarak kullanılmaktadır. Bu çalışmada, yakın fay yer hareketi ile ilişkili olan darbe periyotlarının farklı çapraz konfigürasyonlarına sahip merkezi çaprazlı çerçevelerin üzerindeki etkisini ortaya koymak için zaman tanım alanında dinamik analizler gerçekleştirilmiştir. Bununla birlikte, farklı çapraz konfigürasyonlarının yakın fay yer hareketi altındaki davranışlarının değerlendirilebilmesi için uzak fay yer hareketleri de dikkate alınmıştır. Özellikle küçük, orta ve uzun darbe periyotlarına sahip yakın fay yer hareketleri altında farklı merkezi çaprazlara sahip çelik çerçevelerin dinamik tepkilerini elde etmek için farklı çapraz konfigürasyonlarına sahip 3 katlı ve 4 açıklıklı merkezi gergili çerçeveler uygulama çalışması olarak seçilmiştir. Merkezi çaprazlı çerçevelerin dinamik tepkisini değerlendirmek için farklı darbe sürelerine sahip 4 uzak fay ve 12 yakın fay yer hareketi kullanılmıştır. Sonuçlar, en büyük yer ivmesi değerinin (PGA) uzak fay yer hareketleri altında çaprazlı çerçevelerin tepkisini kontrol eden bir anahtar parametre olarak tanımlanabileceğini göstermiştir. Yakın fay yer hareketlerinde ise darbe periyodunun birinci mod titreşim periyoduna oranının (T_P/T_1) sadece 1.0 değerinden büyük olduğu durumlarda etkin parametre olduğu belirlenmiştir.

Anahtar kelimeler: Dinamik davranış, darbe periyodu, yakın fay, merkezi çapraz, çelik çerçeveler.

1. Introduction

Several research has been carried out to assure the safety of steel building structures exposed to lateral loads like earthquakes and winds, in recent years. Different studies have been carried out for steel frame systems according to these studies. One of the most common of these applications accepted by the current seismic codes is steel braced frames. Braces used in the moment-resisting frame systems (MRFs) are widely used in both concentrically braced frames (CBFs) and eccentrically braced frames (EBFs). A bracing member is used to increase the stiffness of the CBFs laterally axes cross in a single point in the connections between beams. However, the axes in EBFs do not intersect in a single node or point. Elements with large cross-sectional dimensions should be used to ensure adequate rigidity in MRFs. However, in the case of the use of the braces, the stiffness for the

* Corresponding author: hasan.sesli@yalova.edu.tr. ORCID Number of authors: [1] 0000-0002-6637-7949, [2] 0000-0002-3904-3206, [3] 0000-0003-3328-5922

frame systems may be ensured, the displacements and drifts are kept at a desirable level, and also a more economical solution is provided.

When the last decades of studies are surveyed, there are many studies on steel braced frame (SBF) systems. Martinelli et al. [1] investigated the dynamic behavior of CBFs under different earthquake ground excitations. A six-story MRF designed according to Eurocode 8 was analyzed and compared with the results of CBFs. Analysis results showed that CBFs were more effective than MRFs. Balendra and Huang [2] presented a study to determine the ductility and over-strength of split X-braced and reverse V-braced frames designed according to BS5950. As a result of the study, although the over-strength factors and the ductility factors were nearly identical, the response modification factor was reduced depending on the number of stories. Kim and Choi [3] presented a comparative study with reverse V-type CBF and ordinary CBF systems. In the study, ductility, over-strength, and response modification factors were investigated depending on story heights and bays. Dicleli and Mehta [4] studied non-buckling EBFs. To assess the performance of non-buckling EBFs, time history and static pushover analysis were executed. The results of the analysis were compared to the results of CBFs. It is obtained that non-buckling EBFs have less damage than CBFs. Khandelwal et al. [5] used a verified computational simulation on a 10-story building to investigate the progressive collapse resistance of SBFs. Their study showed that the CBF is sensitive to progressive collapse compared to the EBF. Coffield and Adeli [6] studied the structural response of 3D SBFs under blast loading. In the comparative study, three different frame systems were considered, such as MRF, CBF, and EBF. Shiravand and Shabani [7] investigated nonlinear dynamic analysis of 3D structural models of special moment frames, CBFs, and EBFs with 10, 5, and 3 stories under blast loadings. The performance levels, ductility ratios, plastic hinge rotations, and flexural moments obtained from the analysis compared with each other. The results of the analysis showed that EBFs are generally more effective than other systems under burst loads. Qi et al. [8] investigated the seismic performance of EBFs with K-shape and V-shape braced systems designed regarding the Chinese Seismic Design Code. Although V-shape braces were more effective for seismicity, K-shape braces were found to have a lower capacity against seismic loadings. Larijan et al. [9] assessed the developing collapse of steel buildings along with CBF and EBF. Braced bays were investigated for bay numbers and the locations of braces. It has been obtained that the X-braced and reverse V-braced frame systems offer a better strength capacity for progressive collapse, according to a study of both two and three braced bays in the external frames. Bosco et al. [10] proposed a design procedure for MRF and EBF according to Eurocode 8, and dynamic analysis was performed to develop the procedure for buildings founded on soft and hard soil. Karsaz and Tosee [11] examined the seismic performance of 5, 10, and 15-story steel buildings using braces with MRF and different CBF under different earthquake ground excitations. The analysis result showed that X-braced systems have better performance for initial stiffness and yield stress for low-rise buildings, whereas mid-and high-rise buildings with EBF have the least damage and higher ductility performance under an earthquake. It has been observed that the performance of the building with EBF will increase when the story heights are increased. Yaman and Ağcakoca [12] determined the structural performance of some types of CBF shear walls having regular and irregular geometry in steel buildings. It has been observed that the diagonal CBF steel system has more energy absorption capacity than the reverse V-braced shear wall system. Faroughi et al. [13] examined the effects of the number and the location of the braced bays. Nonlinear analysis was performed on five- and eight-story buildings. It has been shown that the number of bays is less effective than the position of braced bays in terms of redundancy and the height of the building is effective in determining the number of braced bays. Additionally, it is not advised to place the bracing solely around the outside of the plan for dual structural systems. Altan [14] performed a static and dynamic analysis of CBF and EBF systems having 5, 10 and 15-story steel structures defined in the Turkish Earthquake Code 2018. It is concluded that eccentrically reverse V-braced systems are more effective than the other bracing systems for stiffness and ductility. Yao et al. [15] aimed to the enhancement of the energy dissipation capacity of prefabricated tension-only concentrically braced beam-through frames (BTFs). The effects of link length, link section, and bracing angle are investigated on seven full-scale eccentrically braced BTFs. Short links improved the load capacity and stiffness of frames, whereas the increment in bracing angle leads to reduce ductility. Haji et al. [16] investigated a new type of EBF and proposed the truss-shaped brace. It is concluded from the analysis that the hollow square cross-sections are very effective for strength and dissipation of energy. Barbagallo et al. [17] investigated the behavior of anti-buckling braces and bi-stage yield buckling braces of CBF and EBF designed according to Eurocode 8. Rouhi and Hamidi [18] used a performance-based plastic design to investigate the influence of forward-directivity on EBFs. To that end 6, 12, and 18-story EBFs were analyzed under NF ground excitations using ETABS software. Allowable drift limits of the EBF frames designed according to the current code were exceeded under NF earthquakes with a forward directivity effect. Gürsoy and Yılmaz [19] investigated the behavior of different EBFs and MRSFs under earthquake excitation. As a result of their study, they showed that models with EBFs are safer than MRSFs.

The results of these research studies showed that although analyses were conducted using various CBFs, the behavior of these frame systems subjected to NF has not comprehensively been studied yet. In this study, aiming to fill this gap, different types of CBFs [20] and MRFs were investigated under ordinary FF ground excitations and NF ground excitations with variable pulse durations. The analysis results of the models having different braced arrangements have been compared for three types of NF and one type of FF earthquake motion sets.

2. NF Ground Motions

One of the most significant dynamic stresses on buildings is strong ground excitation. For the structures, the effects of its characteristics are much more important than the magnitude of an earthquake. Its effects depend on variables such as the amplitude, duration, and frequency content of the ground excitation, as well as the mass of the structure, the natural period, damping, and stiffness. Ground excitations in the NF region can differ greatly from those of FF earthquakes further away from the epicenter.

NF ground excitations are defined as ground vibrations that take place within 20 kilometers of the rupture [21-24]. The velocity pulse duration must be larger than 1.00 seconds and also the ratio of the peak ground velocity (PGV) to the peak ground acceleration (PGA) must be larger than 0.10 seconds [25]. The permanent ground displacements and long-period pulses seem obvious in NF ground excitations. This feature is not visible in recordings gathered in FF regions [26].

NF ground excitations can be categorized as having or not having a pulse signal. Because it is simpler to recognize the pulse from the velocity waveforms, they are used to identify the pulse signals [27]. Figure 1 depicts velocity time series for comparing the NF ground excitation with and without a pulse signal.

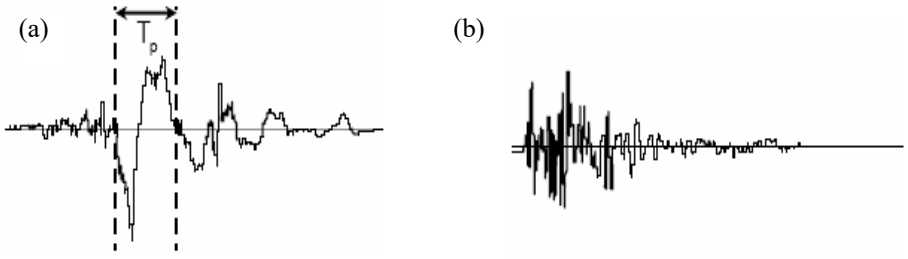

Figure 1. Velocity time series with a pulse (a) and without pulse (b) signals.

Fundamentally, the important response parameters for the structures are the peak values of ground displacement (PGD), velocity (PGV), and acceleration (PGA). NF ground excitations with long-period pulses have a high PGV/PGA ratio, which significantly impacts their responses [28]. The pulse amplitude and duration increase displacements and drift demands. When compared to FF movements, the velocity-sensitive spectral region for NF recordings is substantially narrower, while the acceleration-sensitive and displacement-sensitive sections are much wider. NF ground excitations required a greater strength demand than FF motions for the same ductility factor. The reaction for both NF and FF ground movements became identical if the periods were normalized to the transition time of the acceleration-sensitive area [29]. Resonance can considerably increase the demands on a structure if the pulse period and the fundamental period of the structure are aligned [30]. Much demand can be required for a structure under a large number of remarkable cycles. Fortunately, only one or two remarkable cycles occur mostly in the case of forward-directivity. The pulse period is the period at which the ratio of the spectral velocity of the peak-to-peak velocity (PPV) pulse to the median spectral velocity from the Next Generation Attenuation (NGA) models is at a maximum [31]. PPV is also the difference between the two peaks in a single motion cycle.

T_p/T_1 is a critical number which is a ratio of the pulse duration to the first mode period for specifying the structural response under NF ground excitations with pulse or pulse-like motions [27,32-33]. Although the earthquake motion records with T_p/T_1 have larger mode effects and maximum reaction at higher stories, the short period structures under the records with a large pulse have a maximum ductility demand in bottom stories [32].

In the present study, an MRF and different types of CBFs given in TBEC-2018 [20] were subjected to two types of ground excitation records, which are NF ground excitation having different pulse durations and ordinary FF records. The period of the pulse (extracted pulse, T_p) is identified as the time needed to complete a full velocity cycle and is obtained in the velocity time history (VTH) of the selected ground excitations. The duration of extracted pulse period is considered by selecting a proper NF ground excitation and selected motions are also

classified sets as large, medium, and small pulses as shown in Table 1. The large, medium and small pulse periods are respectively over 3 sec., a range of about 1.5 sec. and about 2.9 sec., and smaller than about 1.2 sec. Besides, every record set given in Table 1 which contained three types of NF and one type of FF earthquake motion, which are nearly the same PGV/PGA.

In addition, the original VTH of ground excitations with the associated extracted pulses for all types of selected motions are given in Figures 2-4. The pulse velocities associated with selected motions are drawn [34] software according to the method proposed by Kardoutsou et al. [35]. It can be seen easily in Figure 2 that the extracted pulse for NF small pulse covers substantially the entire time history as compared to the NF medium (Figure 3) and NF large (Figure 4) pulses.

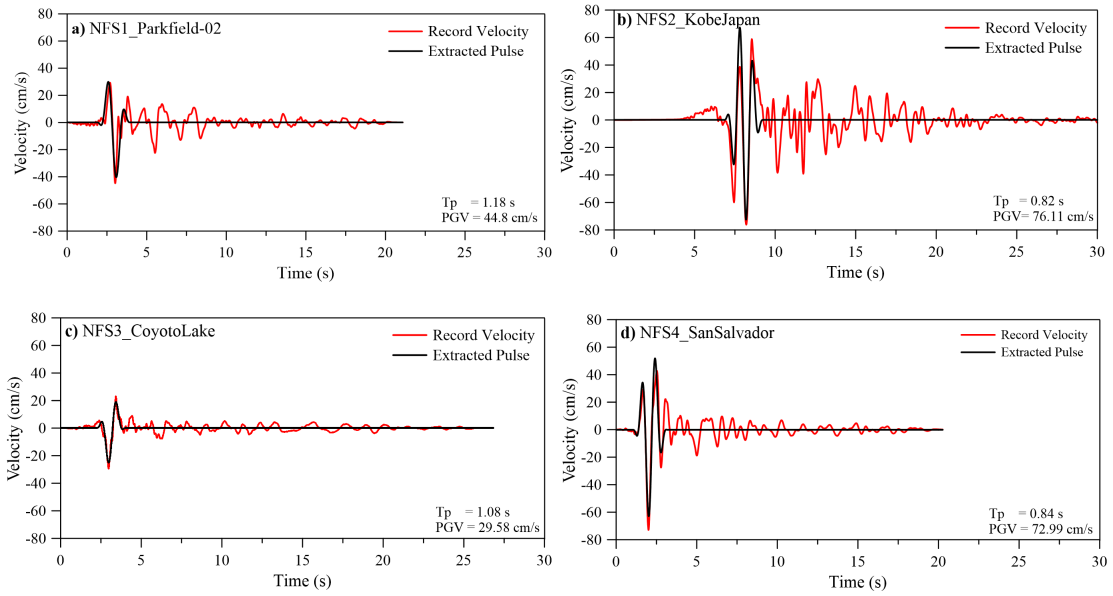

Figure 2. VTHs of NF small pulse.

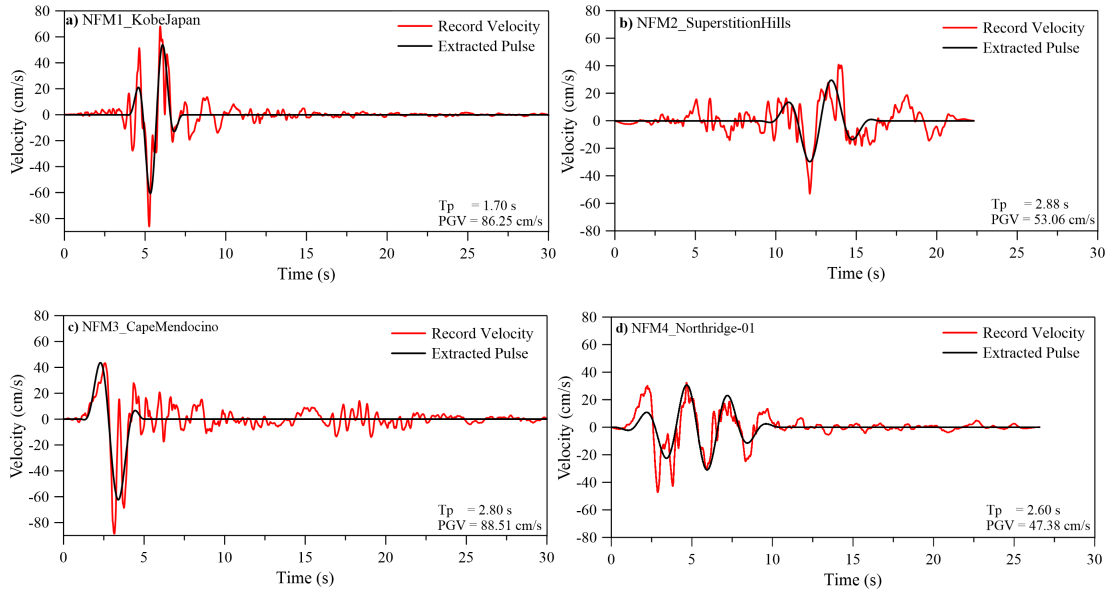

Figure 3. VTHs of NF medium pulse.

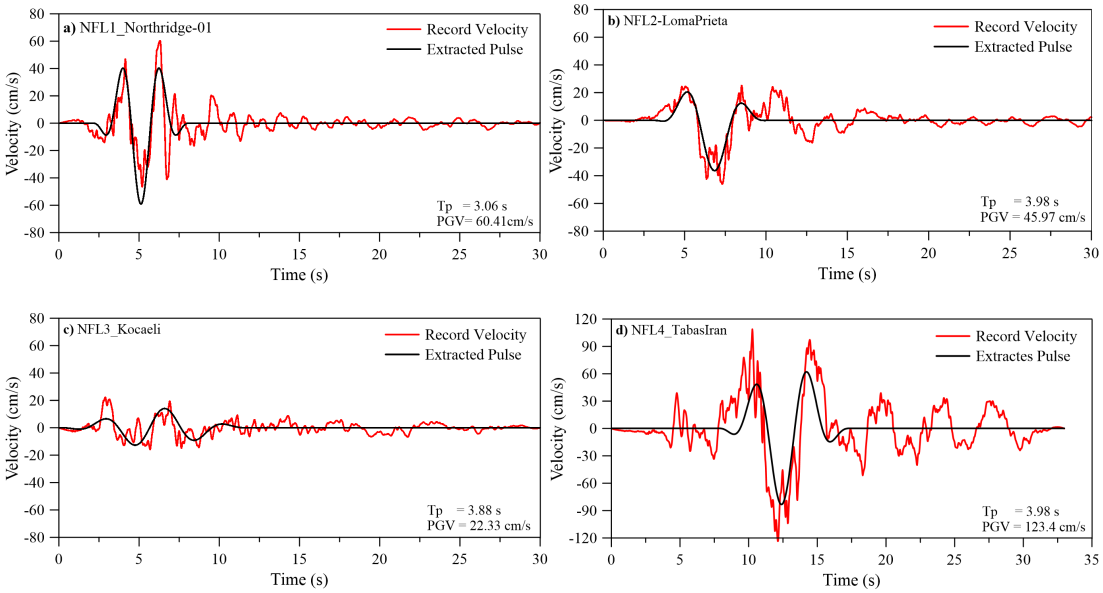

Figure 4. VTHs of NF large pulse.

Table 1. Dynamic characteristics of selected ground motions [36]

Motion Type	*RSN*	*Earthquake*	M_w	*Station*	R_{rup} *(km)*	*PGA (g)*	*PGV (cm/s)*	$\frac{PGV}{PGA}$	T_p *(sec)*
*NFL**	1085	Northridge-01	6.69	Sylmar - Converter Sta East	5.19	0.449	60.41	0.14	3.06
	802	Loma Prieta	6.93	Saratoga - Aloha Ave	8.50	0.326	45.97	0.14	3.98
	1165	Kocaeli, Turkey	7.51	İzmit	7.21	0.165	22.33	0.14	3.88
	143	Tabas, Iran	7.35	Tabas	2.05	0.862	123.4	0.15	3.98
*NFM**	1013	Northridge-01	6.69	LA Dam	5.92	0.324	47.38	0.15	2.60
	1119	Kobe, Japan	6.90	Takarazuka	0.27	0.614	86.25	0.14	1.70
	723	Superstition Hills-02	6.54	Parachute Test Site	0.95	0.384	53.06	0.14	2.88
	828	Cape Mendocino	7.01	Petrolia	8.18	0.662	88.51	0.14	2.80
*NFS**	4100	Parkfield-02, CA	6.00	Parkfield - Cholame 2WA	3.01	0.373	44.80	0.12	1.18
	1106	Kobe, Japan	6.90	KJMA	0.96	0.630	76.11	0.12	0.82
	569	San Salvador	5.80	National Geografical Inst	6.99	0.534	72.99	0.14	0.84
	148	Coyote Lake	5.74	Gilroy Array #3	7.42	0.256	29.58	0.12	1.08
*FF**	491	Taiwan SMART1(33)	5.80	SMART1 O01	41.99	0.049	2.02	0.04	-
	5802	Iwate, Japan	6.90	Yokote O Morimachi	44.86	0.219	8.49	0.04	-
	6949	Darfield, New Zealand	7.00	PEEC	53.75	0.117	4.59	0.04	-
	436	Borah Peak, ID-01	6.88	CPP-601	82.60	0.040	1.60	0.04	-

NFL NF ground motions (large-pulse period)*
NFM NF ground motions (medium-pulse period)*
NFS NF ground motions (small-pulse period)*
*FF *FF ground motions*

3. Structures Description and Modeling

The geometric details of the structures considered for linear time-history analyses are demonstrated in Figure 5. The MRF system is expressed as an unbraced frame system in this study. The different five frame types [20] were selected and designed according to AISC360-16 [37]. Each model has three stories and 4-span in the x-

direction, the span length and the story height are 6 m and 3 m, respectively. The dynamic analyses were carried out using SAP2000 [38] under FF and NF earthquake ground excitations considered models of the study. The models consist of an unbraced frame system and the five braced models of CBFs defined in [20]. The braces are located on the two side spans of the structure in CBFs as shown in Figure 5. The frames are represented on the x-z plane since the linear time history analyses are done in plane. The profile sections used are given in Table 2. Young's modulus was taken as 2.1×10^5 MPa. S275 [37] steel material type was used in the considered models.

Table 2. Section details for the model

Story	*Beam*	*Column*	*Diagonal*
1	HE120A	HE140A	HE120A
2			
3			

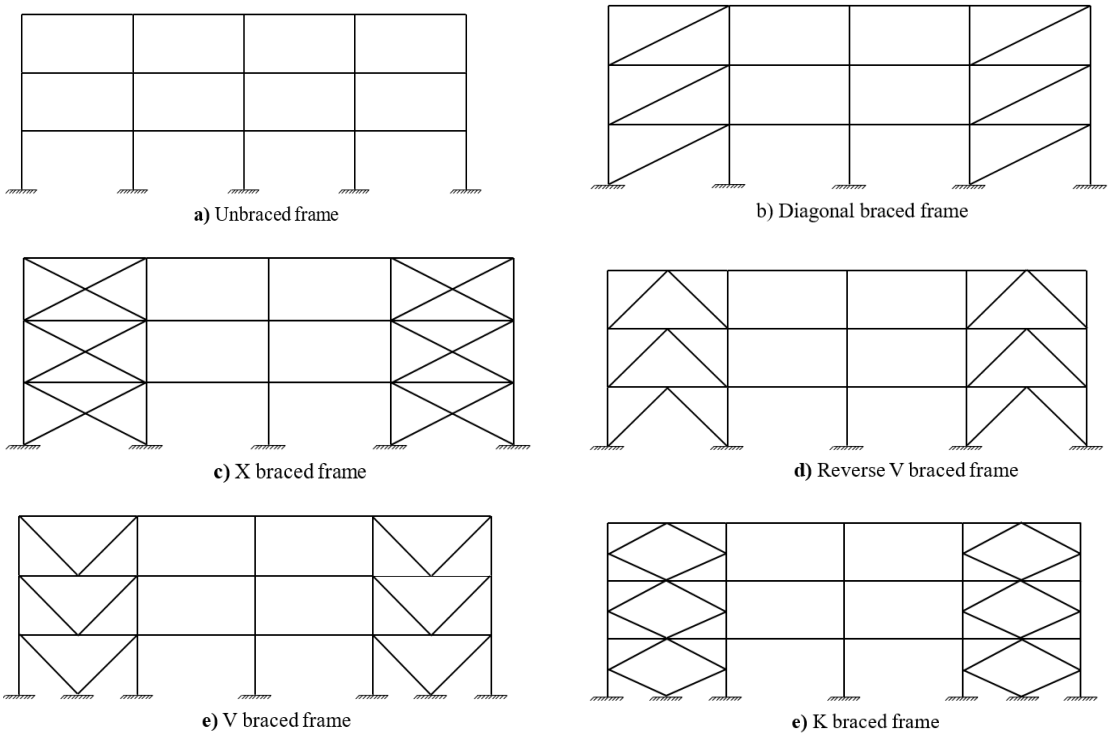

Figure 5. Typical unbraced and concentrically braced steel frame systems.

4. Results and Discussion

Firstly, the behavior of the unbraced steel frame system subjected to four different ground excitations categories consisting of NF and FF was investigated. As a result of the modal analysis, the fundamental period values of the unbraced steel frame and structural models having different steel braced types, performed according to the mode coupling method are given in Table 3.

The unbraced frame system has the largest dominant period while the reverse V-braced frame system has the smallest period as can be seen from Table 3. This shows that the period values are significantly reduced with the use of brace elements in the structural models. This finding shows that the period values of the steel braced frame models decrease with the increase in the rigidity of the structure caused by using steel brace elements.

As a part of the analysis's results interpretation, NFL, MFM, and NFS abbreviations used in the figures are NF large pulse, NF medium pulse, and NF small pulse, respectively. The maximum floor displacements of the unbraced frame system under the earthquake categories are given in Figure 6. The maximum story displacements that were obtained under the Iwate-Japan earthquake ground excitation were higher than those of other ground excitations, as can be seen from Figure 6-a. The other FF ground excitations with much smaller PGA values

compared to the Iwate-Japan earthquake motion (PGA=0.219g) record caused very small displacements close to each other. By examining four NF records with small pulses (NFS), the Kobe-Japan earthquake record motion having a higher PGA value (0.630g) has a noticeable effect on the story displacements (Figure 6-b). All results of the NF effects are much greater than FF ground excitations. The parameter PGA of the motions has been very effective than pulse duration (T_P) and PGV/PGA values for the displacements. Therefore, the maximum story displacement values are obtained from Kobe-Japan, San-Salvador, Parkfield-02, and Coyote-Lake earthquakes for NFS pulses, respectively. For category NFM (Figure 6-c), the higher displacements are obtained from Kobe-Japan earthquake record motions with smaller pulse duration. Since the PGA values of the Northridge-01 and Superstition-Hills earthquake record motions are smaller than the Kobe-Japan and San-Salvador earthquake motions, which have also the largest pulse duration less maximum story displacements are obtained compared to other earthquakes. Considering Figure 6-d, in the Tabas-Iran earthquake having a greater PGA value (0.862g), the maximum and the largest story displacements occurred. Although the Kocaeli Earthquake has a large impact duration, braced frame systems are subject to smaller storey displacements under the Kocaeli earthquake, which has a smaller PGA (0.165g) than other earthquake ground excitations.

Table 3. The periods depend on the vibration modes of the considered models

Models	*Fundamental Period (sec.)*		
	1st Mode	*2nd Mode*	*3rd Mode*
Unbraced frame	0.3615	0.1076	0.0583
Diagonally braced frame	0.0540	0.0190	0.0156
X-braced frame	0.0404	0.0168	0.0166
Reverse V-braced frame	0.0368	0.0160	0.0150
V-braced frame	0.0454	0.0169	0.0164
K-braced frame	0.0407	0.0325	0.0325

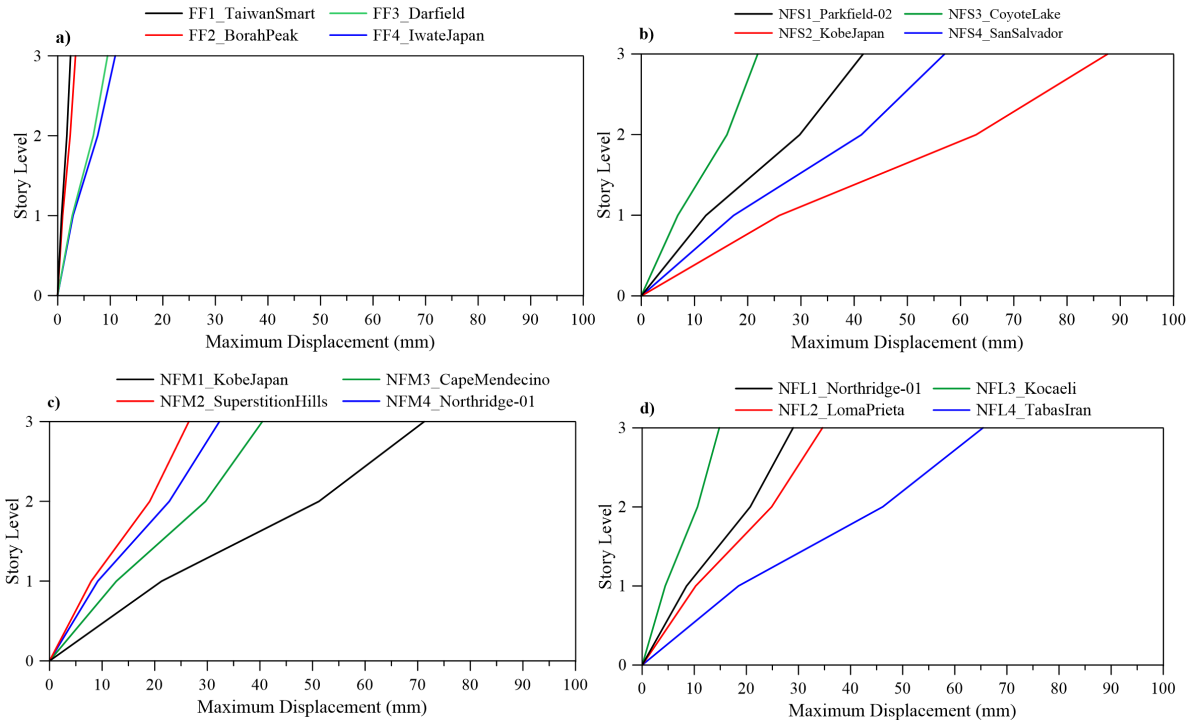

Figure 6. Maximum lateral displacement for the unbraced frame system.

Iwate-Japan earthquake ground excitation, which has higher results than those of other FF ground excitations. The other FF ground excitations having much smaller PGA values as compared to the Iwate-Japan earthquake motion record caused very small displacements and have close displacements. By examining NFS pulse results (Figure 7-

b), although the story displacements up to the 2nd story are close to each other in the Kobe and Salvador earthquakes, they are different at the 3rd story. While the largest story displacement in the unbraced system is in the Kobe earthquake, the story displacements in the diagonal frame system are close to each other. By examining NFM pulse results (Figure 7-c), the Cape Mendocino earthquake record motion having a higher PGA value has a noticeable effect on the story displacements. All results are nearly greater than FF ground excitations. Therefore, the maximum story displacement values are obtained from Cape Mendocino, Kobe Japan, Superstition Hills, and Northridge earthquakes, respectively. While the largest story displacement in the unbraced system is in the Kobe earthquake, the largest story displacement in the diagonal frame system is in the Cape Mendocino earthquake. It can be depicted from Figure 7-d that the Tabas-Iran earthquake having a greater PGA gave larger maximum story displacements for the diagonal steel frame system. The PGA values have been very effective than pulse duration for the story displacements. Besides, the maximum story displacement values are obtained from Tabas-Iran, Northridge, Loma Prieta, and Kocaeli earthquakes, respectively. As in the unbraced system, the largest story displacement is observed in the Iran Tabas earthquake.

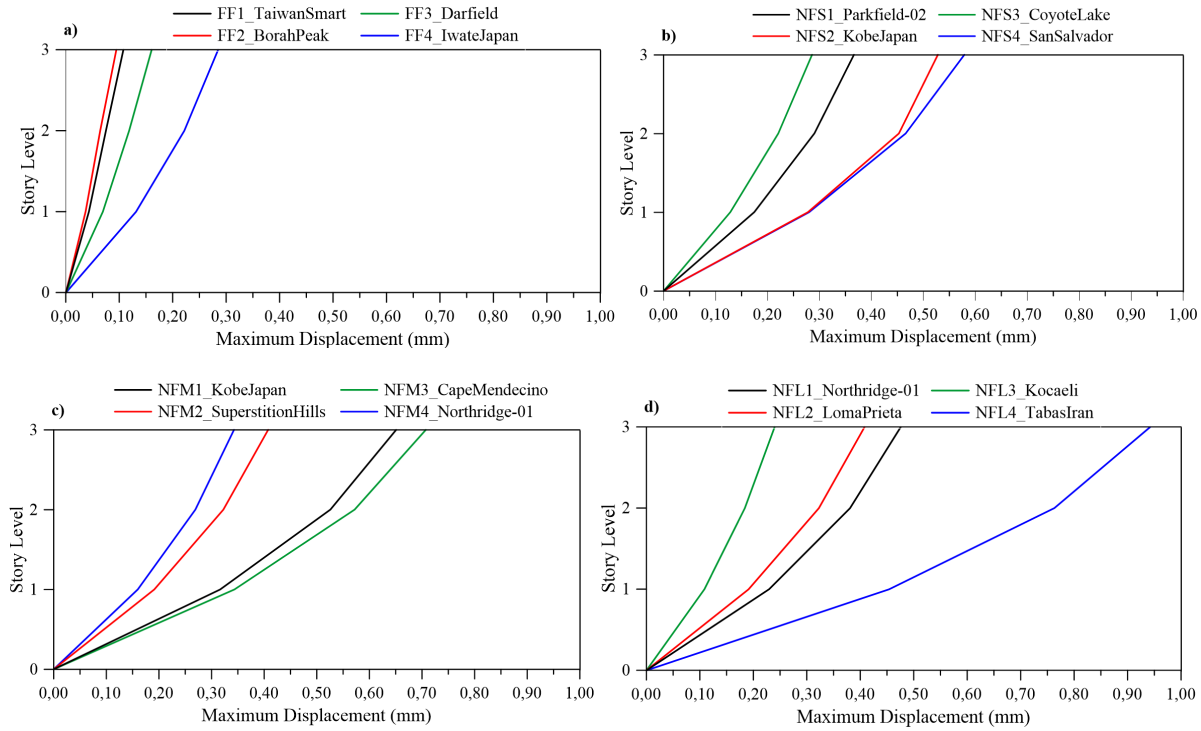

Figure 7. Maximum lateral displacement for the diagonally braced frame system.

The maximum story displacements for the X-braced frame are given in Figure 8. As it can be seen from Figure 8-a, the maximum story displacements of the X-braced frame system are obtained under the Iwate-Japan earthquake for FF ground excitations. The other FF ground excitations having much smaller PGA values compared to the Iwate-Japan earthquake record caused very small displacements and have close displacements. By examining NFS pulse results (Figure 8-b), the maximum story displacement occurred Kobe Japan earthquake having the biggest PGA in the X-braced frame system. The PGA values have been very effective than pulse duration for the story displacements. The story displacements in the X-braced frame are quite small compared to the unbraced system. In the NFM pulse results (Figure 8-c), the Cape Mendocino earthquake record motion having a higher PGA value (0.662g) has been quite effective on the maximum story displacements. All results for NF are much greater than FF ground excitations. Having nearly the same PGV/PGA motions, the maximum story displacement values are obtained from Cape Mendocino, Kobe Japan, Superstition Hills, and Northridge earthquakes, respectively. While the largest story displacement in the unbraced system is in the Kobe earthquake, the largest story displacement in the X-braced frame system is in the Cape Mendocino earthquake. It can be depicted from Figure 8-d that the Tabas-Iran earthquake having a greater PGA result in larger story displacements for the X-braced frame system. Also, the maximum story displacement values were obtained from Tabas-Iran,

Northridge, Loma Prieta, and Kocaeli earthquakes, respectively. As in the unbraced system, the largest story displacement is observed in the Tabas-Iran earthquake in the X-braced frame system.

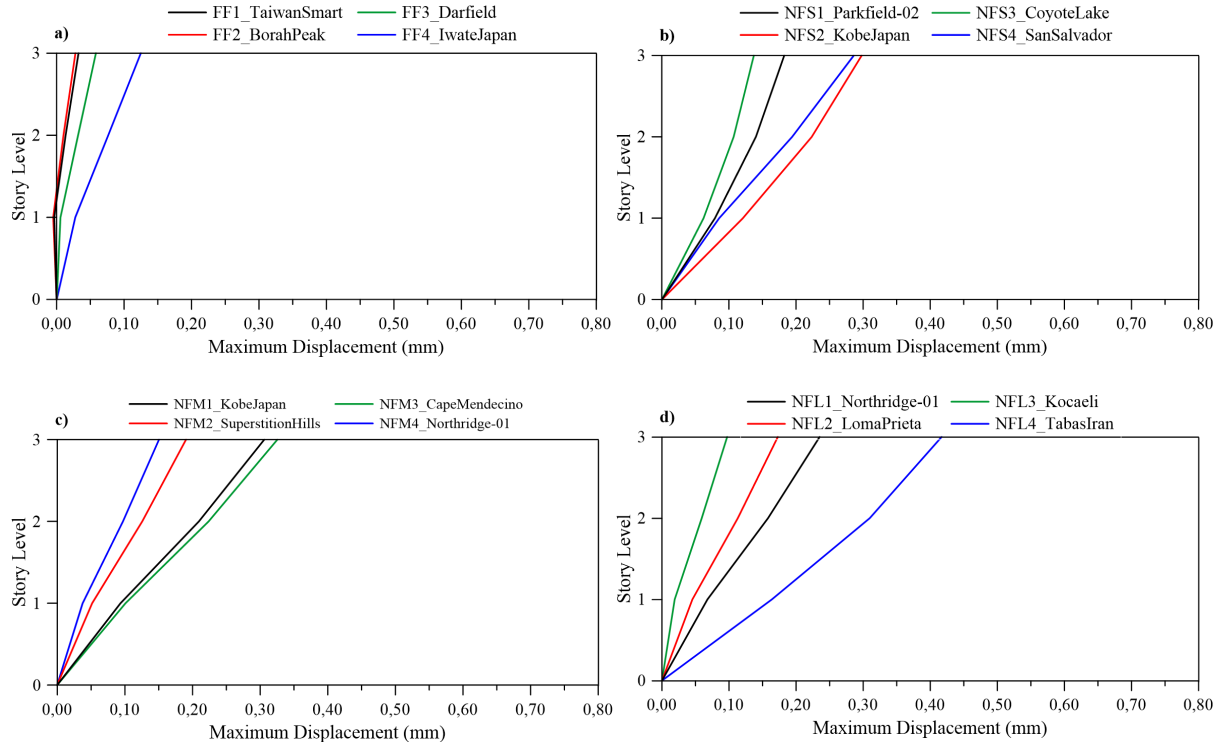

Figure 8. Maximum lateral displacement for the X-braced frame system.

The variation of lateral displacements at every floor level of the reverse V-braced steel frame system is presented in Figure 9. As can be seen in Figure 9-a that the maximum displacements occur under Iwate-Japan earthquake ground excitation like in the unbraced frame, whereas the Darfield-New Zealand earthquake lost effects on the lateral displacements. When the reverse V-braced steel frame system is subjected to four NF records with NFS pulse in Figure 9-b, it is clear that the lateral displacements obtain from the Kobe-Japan and the San Salvador earthquakes, which caused a larger displacement and had less pulses, come close to the lateral displacements obtained from the Parkfield-02 and Coyote-Lake record motions. Figure 9-c shows that the Superstition-Hills and Cape-Mendocino earthquake record motions which had large velocity pulse duration were very effective compared to the unbraced frame. However, the Kobe-Japan earthquake which caused larger displacements on the unbraced frame has not had larger displacements since it had a smaller velocity pulse duration. It can be depicted from Figure 9-d that the Tabas-Iran earthquake having a greater PGA and pulse duration results in larger maximum story displacements for the reverse V-braced steel frame system. Although the displacements obtained from the Loma-Prieta Earthquake have decreased, the lateral displacements for the Northridge-01 earthquake have considerably increased compared to the unbraced frame system.

The maximum story displacement results deal with the V-braced steel frame system under different earthquake motions are presented in Figure 10. Although the similarities observed in the other frames are also seen in this frame, Figure 10-a shows that the Iwate-Japan earthquake ground excitation greatly increases efficiency in the V-braced frame compared to the others. From Figure 10-b, it is observed that Kobe-Japan has less pulses and larger PGA values cause larger displacements same as the San Salvador earthquake, but it lost effectiveness compared to the unbraced frame system. Figure 10-c illustrated that the Kobe-Japan earthquake, which has a smaller velocity pulse duration, has not larger displacements compared to the unbraced frame, and also the Cape-Mendocino earthquake which has a larger velocity pulse duration and a larger PGA value results in the maximum lateral displacements. It can be seen from Figure 10-d that the Tabas-Iran earthquake having a greater PGA and pulse duration caused the large structural demand for the V-braced steel frame system. The Loma-Prieta

earthquake lost the efficiency of structural behavior of the V-braced steel frame system compared to the unbraced frame system.

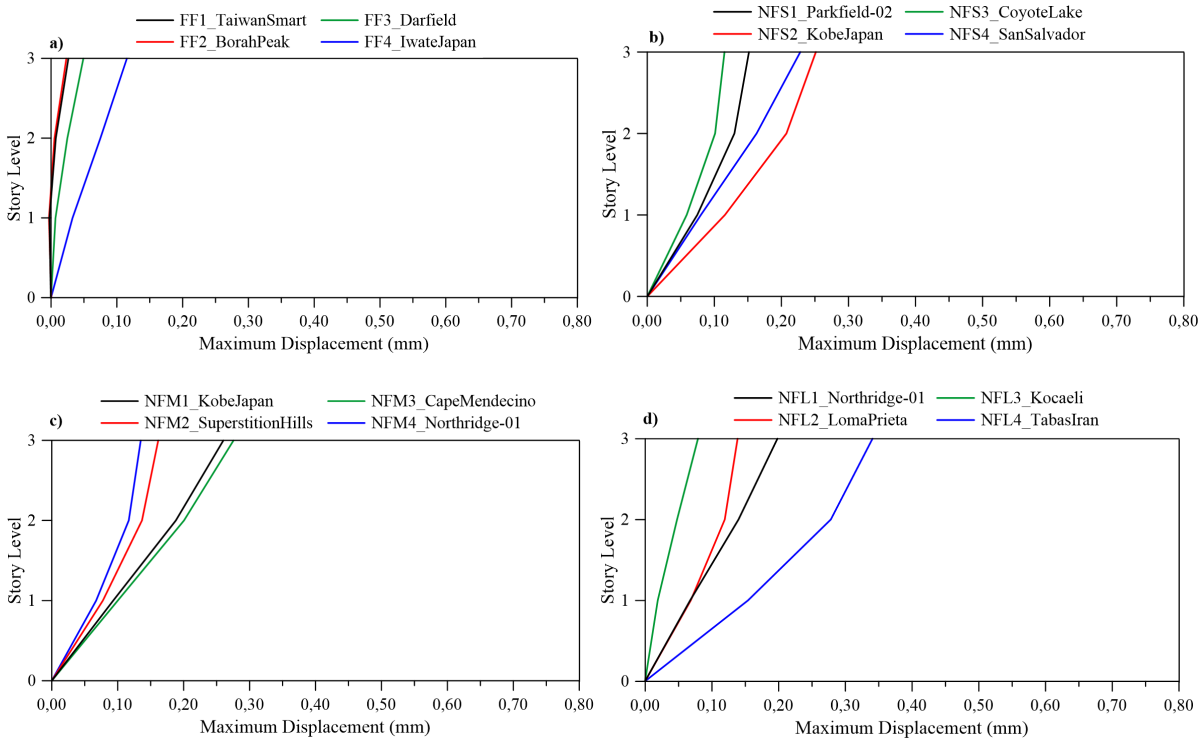

Figure 9. Maximum lateral displacement for the reverse V-braced frame system.

The results of analysis obtained from the K-braced frame system for FF earthquakes showed that the results are obtained as similar to the unbraced frame system, but the Darfield Earthquake gave less lateral displacement compared to the unbraced frame system (Figure 11-a). It can be said that PGA values are very effective for FF earthquakes. The investigation of the lateral displacements of K-braced frame systems under near-fault earthquake motions with small pulse duration present that the Kobe-Japan earthquake which has a small pulse duration compared to the other had less effect on the structural behavior according to the unbraced frame system (Figure 11-b). According to Figure 11-c, the Kobe-Japan earthquake lost the efficiency in structural behavior compared to the unbraced since this motion has a low pulse duration. Whereas the Cape-Mendocino and the Superstition Hills-02 earthquakes have a low effect on the unbraced frame system, these record motions, which have large pulse durations, caused an increase in the displacements of the K-braced frame systems. When Figure 11-d is examined, the Tabas-Iran earthquake is very effective on the structural behavior of the K-braced frame system same as unbraced frame system. The Loma-Prieta Earthquake is not effective on the structural behavior of the K-braced steel frame system compared to the unbraced frame system.

Figure 12 shows the relationship between different frame systems and FF earthquake motions for the maximum displacements of the top floor. When the first-mode periods of vibrations given in Table 3 are considered, all results obtained from six-different frame systems depend on the first-mode periods of vibrations. The Iwate-Japan and the Darfield-New Zealand earthquakes have large PGA values in the FF earthquakes. The maximum top floor displacements are obtained as 10.98 mm, 0.285 mm, 0.125 mm, 0.115 mm, 0.207 mm, and 0.134 mm under the Iwate-Japan earthquake for unbraced, diagonal braced, X-braced, reverse V-braced, V-braced, K-braced, respectively. Similarly, the top floor displacements are as 9.51 mm, 0.16 mm, 0.058 mm, 0.049 mm, 0.097 mm, and 0.062 mm for the Darfield-New Zealand earthquake. The percentage variations in displacements derived from two record motions were 13%, 44%, 54%, 57%, 53% and 54%, respectively. For the FF earthquakes, PGA values and the stiffness are the effective parameters for steel frame systems, and also as long as the stiffness of the system is increased, the structural demands are increased depending on PGA values.

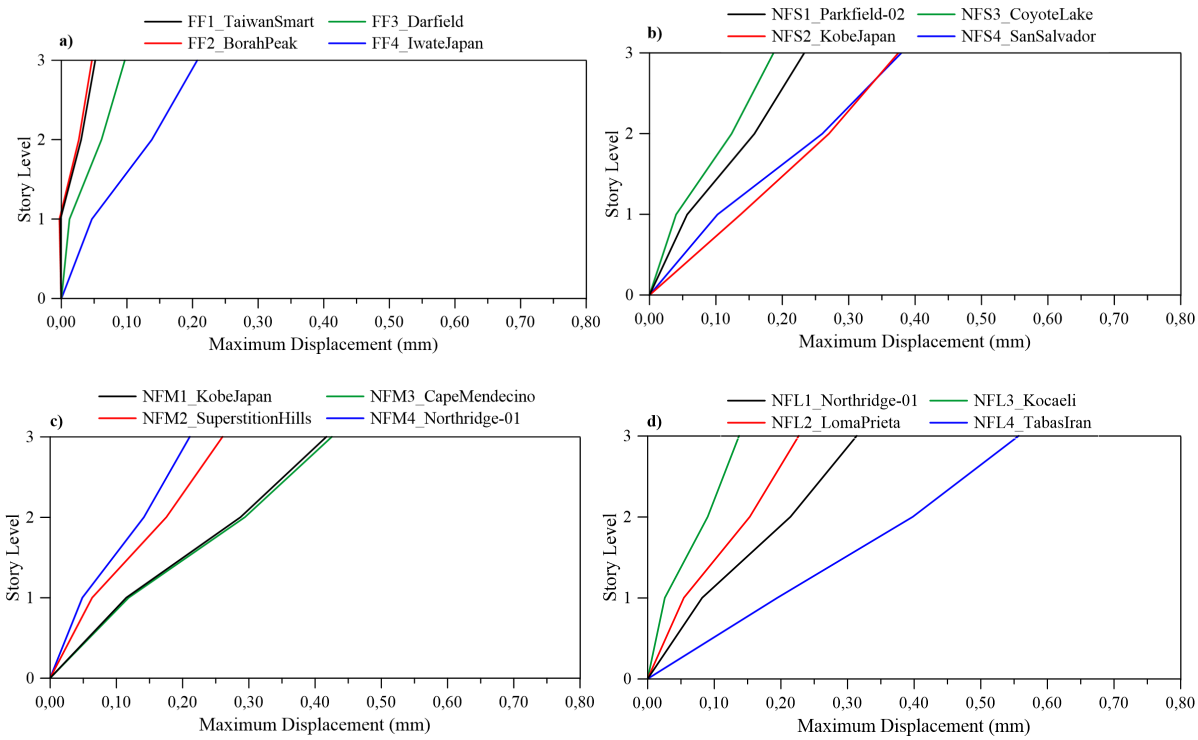

Figure 10. Maximum lateral displacement for the V-braced frame system.

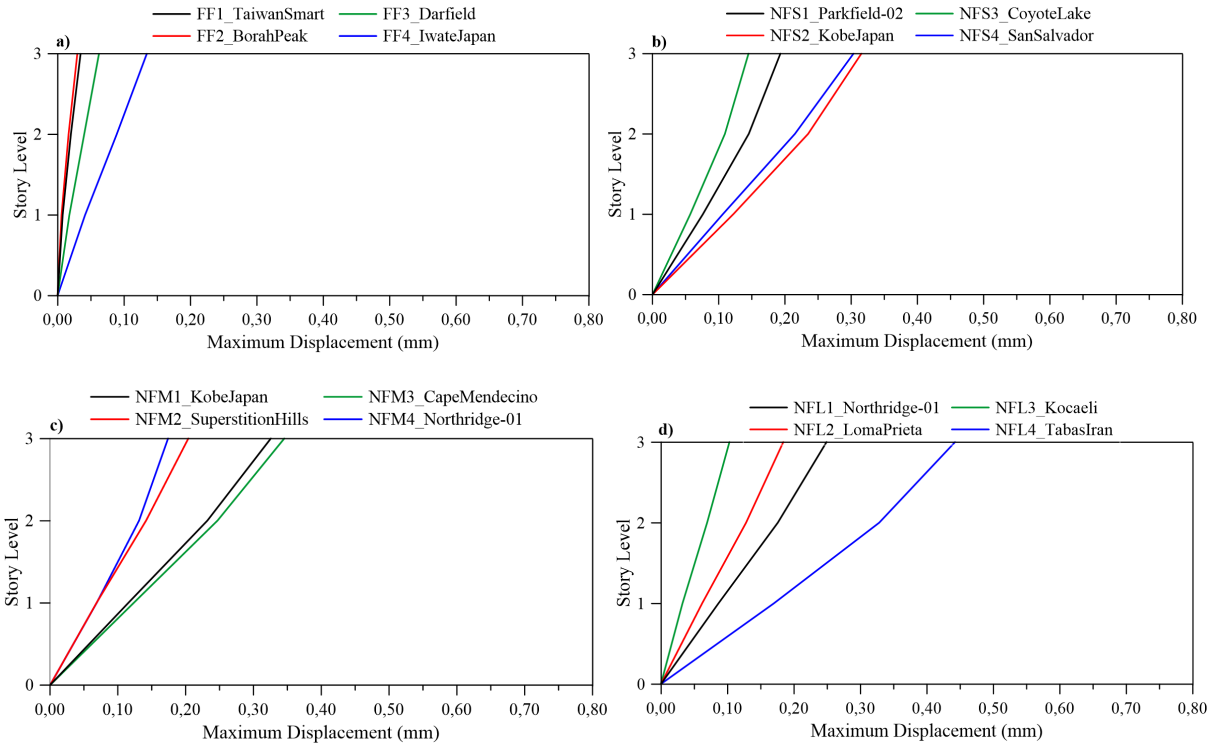

Figure 11. Maximum lateral displacement for the K-braced frame system.

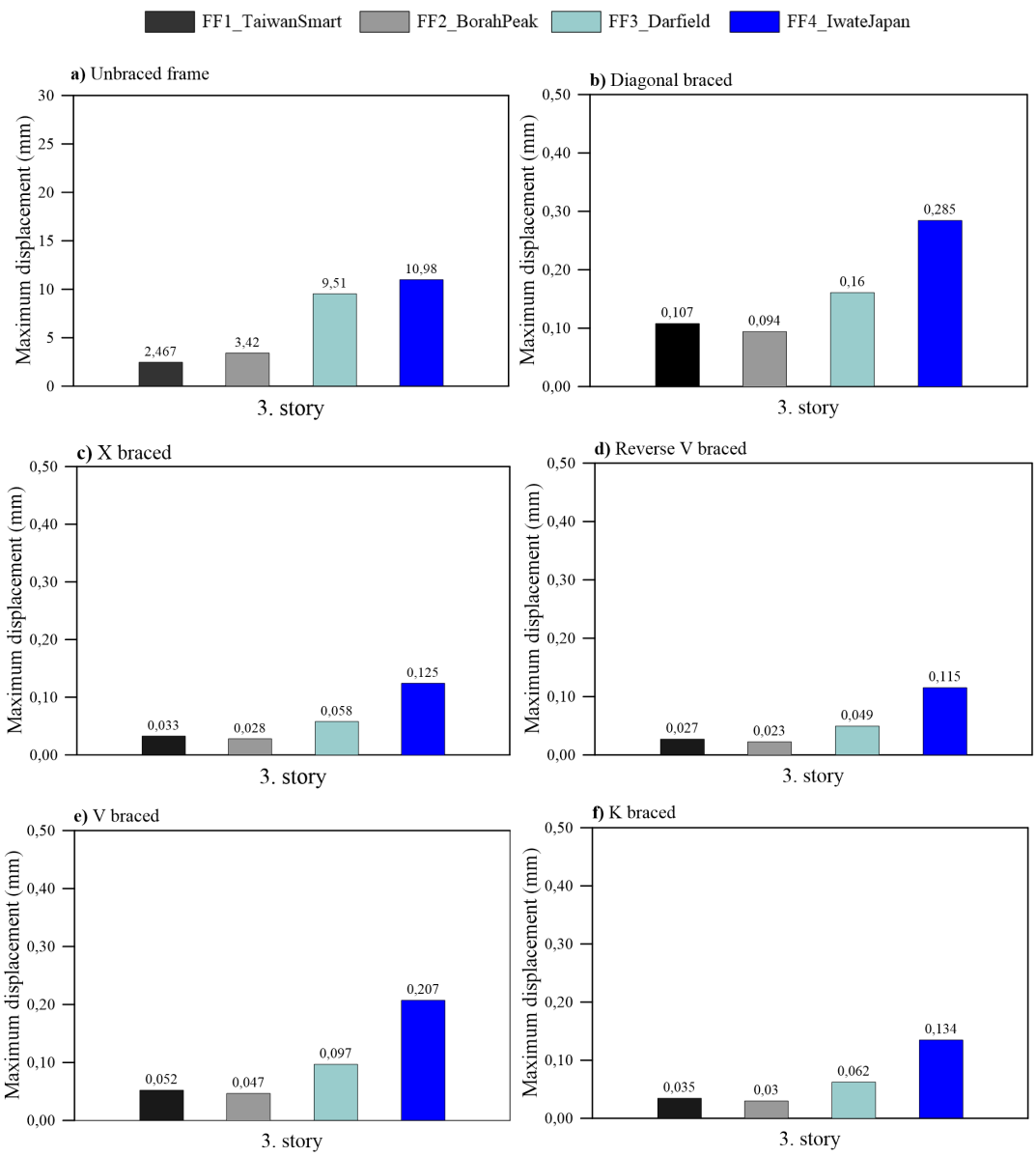

Figure 12. Maximum horizontal displacements considering different bracing models for the FF.

The maximum displacements of top floors for the considered models are compared according to NFS pulse duration in Figure 13. Kobe-Japan and San-Salvador earthquakes have both large PGA values and lower pulse duration compared to other earthquakes with small pulses. For this record motions, the variations in displacements are -35%, 9.60%, -4%, -9.20%, 1% and -3.80% according to the results of Kobe-Japan earthquake. When the diagonal braced frame system, which is the more flexible braced system, is compared to the reverse V-braced system, which is a most stiff system, in considering to first mode period, the variation in percentage is 58%, 52%, 60% and 60% for the Parkfield-02, Kobe-Japan, Coyote-Lake, and San-Salvador, respectively. The Kobe-Japan earthquake having a large PGA is very effective on the reverse V-braced system, which is a very stiff braced system. While the unbraced frame system has a 26% variation in the top floor displacements under the Parkfield-02 and San-Salvador earthquakes, the variation in the top floor displacements are 36%, 36%, 33%, 38%, 36% for diagonal, X-braced, reverse V-braced, V-braced and K-braced frame systems, respectively. PGA values are significant parameter in the systems for the NFS pulse motions.

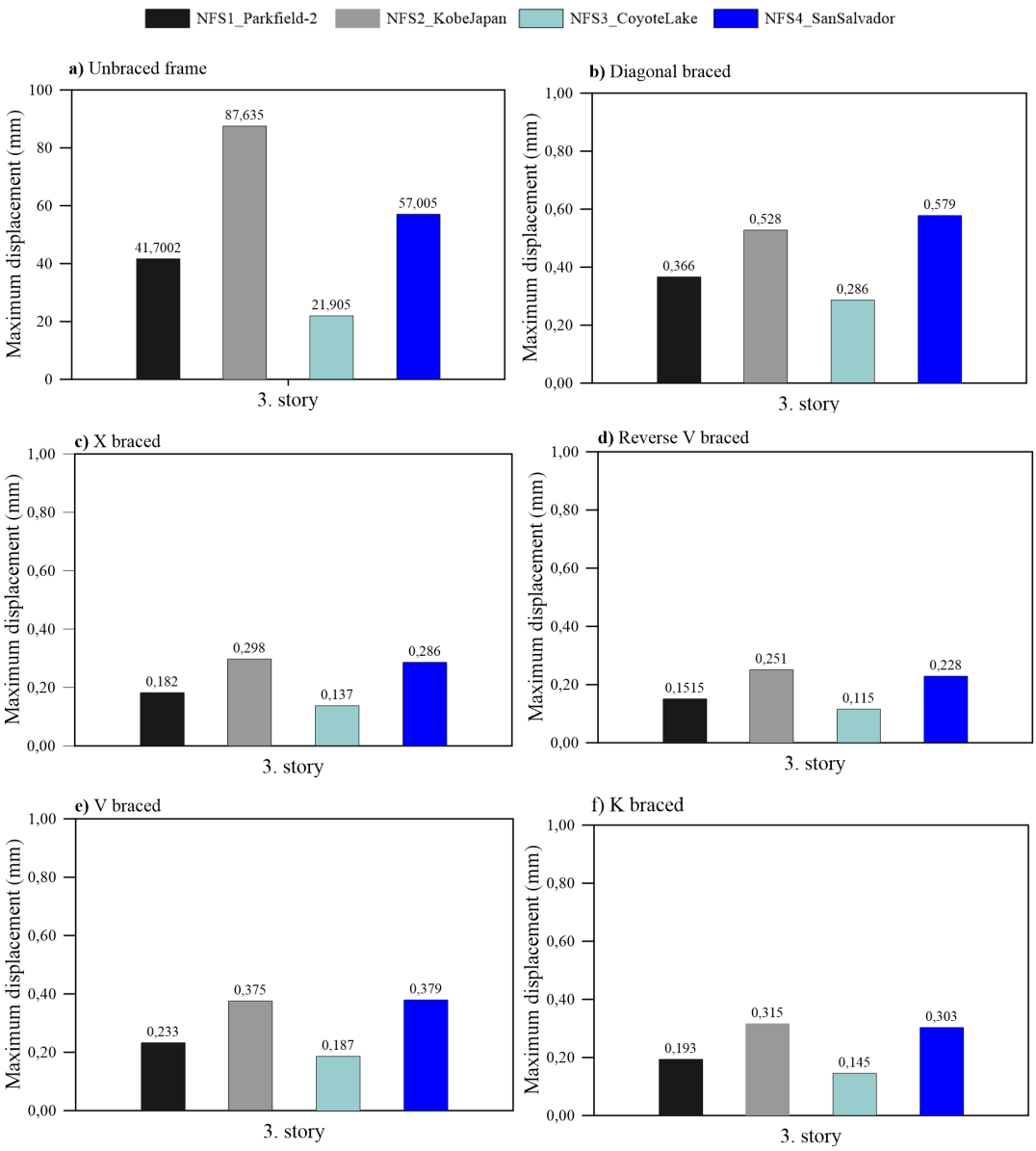

Figure 13. Maximum horizontal displacements considering different bracing models for the NFS.

The effect of NFM pulse motions on the maximum displacements of the top floor for the considered models is compared in Figure 14. The Cape-Mendocino earthquake, which has a larger pulse duration and the Kobe-Japan earthquake has nearly the same PGA values. The variations in displacements obtained from the Cape-Mendocino earthquake according to the Kobe-Japan earthquake are -43.28%, 8.60%, 6.53%, 6.15%, 1.92%, 6.15% for unbraced, diagonally braced, X-braced, reverse V-braced, V-braced, K-braced, respectively. The diagonal braced frame system is very sensitive to the pulse duration. Although a diagonal braced frame system has a large vibration natural period, the V-braced frame system is less affected under pulse duration. Except for the unbraced frame system, all braced frame systems are affected by pulse duration under the Cape-Mendocino earthquake. Furthermore, the Superstition-Hills earthquake is very effective on the braced frame systems compared to the Northridge-01 record motion.

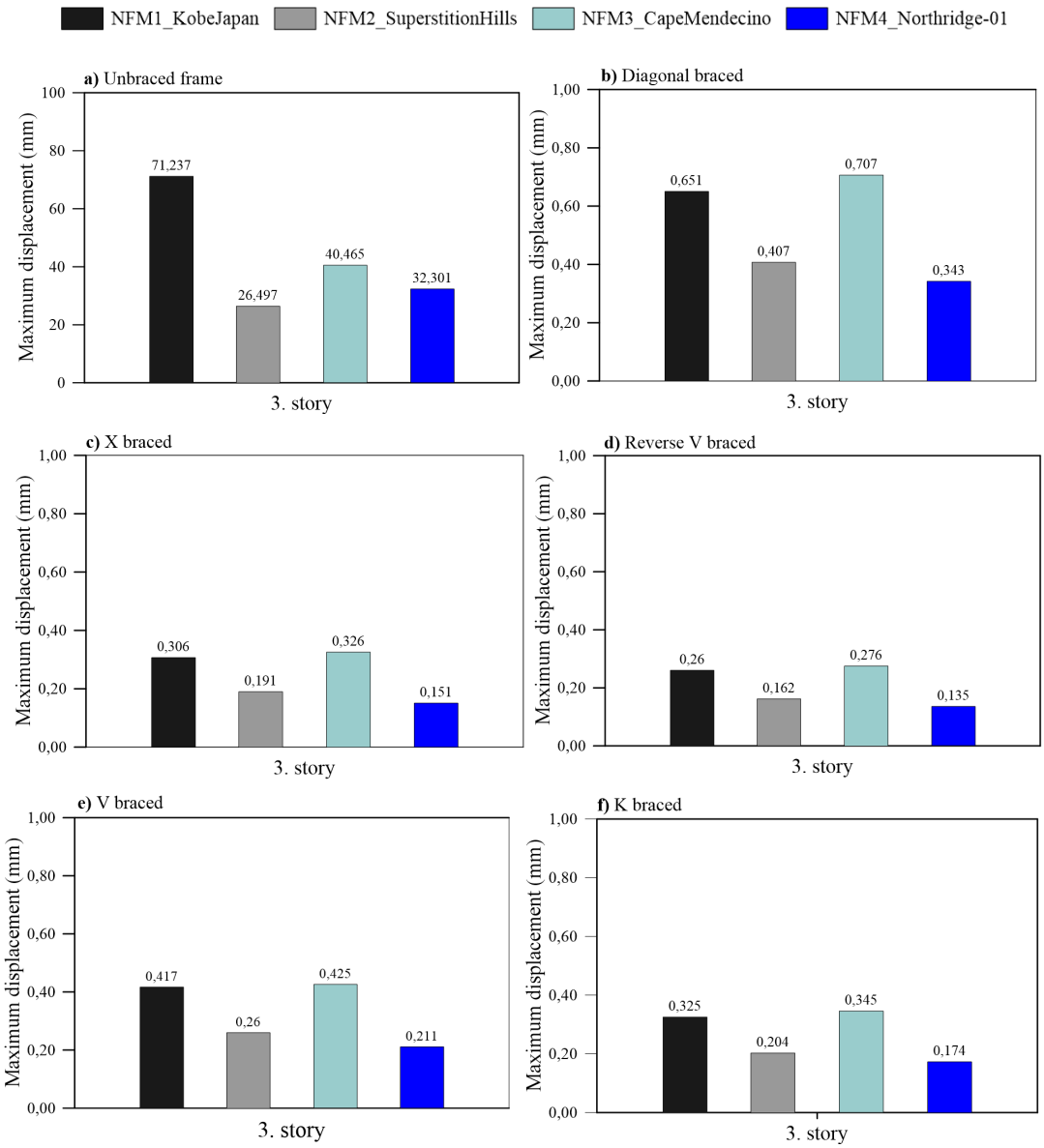

Figure 14. Maximum horizontal displacements considering different bracing models for the NFM.

For the unbraced frame system in Figure 14, the maximum top floor displacements obtained from the Northridge-01 record motion are greater than the displacements obtained from the Superstition-Hills. However, the Superstition-Hills earthquake result in greater maximum displacements compared to the Northridge-01 record motion. Under the Superstition-Hills earthquake, the maximum top floor displacements are 26.497 mm, 0.407 mm, 0.191 mm, 0.162 mm, 0.26 mm, 0.204 mm for the unbraced, diagonally braced, X-braced, reverse V-braced, V-braced, K-braced, respectively. In addition, the maximum top floor displacements are 32.301 mm, 0.343 mm, 0.151 mm, 0.135 mm, 0.211 mm, 0.174 mm under the Northridge-01 record motions, respectively. When the results obtained under the Superstition-Hills and Northridge-01 record motions are considered, the variations are as 21.90%, -15.72%, -20.94%, -16.67%, -18.85% and -14.70% for all systems, respectively. The Superstition-Hills and the Cape-Mendocino earthquakes have nearly the same pulse duration, but these record motions have quite different PGA values. While the top floor displacements are respectively obtained as 26.497 mm, 0.407 mm, 0.191 mm, 0.162 mm, 0.260 mm, 0.204 mm for all frames under the Superstition-Hills earthquake, the top floor displacements were respectively obtained as 40.405 mm, 0.707 mm, 0.326 mm, 0.276 mm, 0.425 mm, 0.345 mm for all frames under the Cape-Mendocino earthquake. The variations in top floor displacements for the Superstition-Hills and the Cape-Mendocino earthquakes are 52.48%, 73.71%, 70.68%, 70.37%, 63.46%, and

69.12% for all systems, respectively. While the unbraced frames have a structural demand under the earthquakes with large PGA values, the structural behavior of the braced systems is increased under the earthquakes with a pulse.

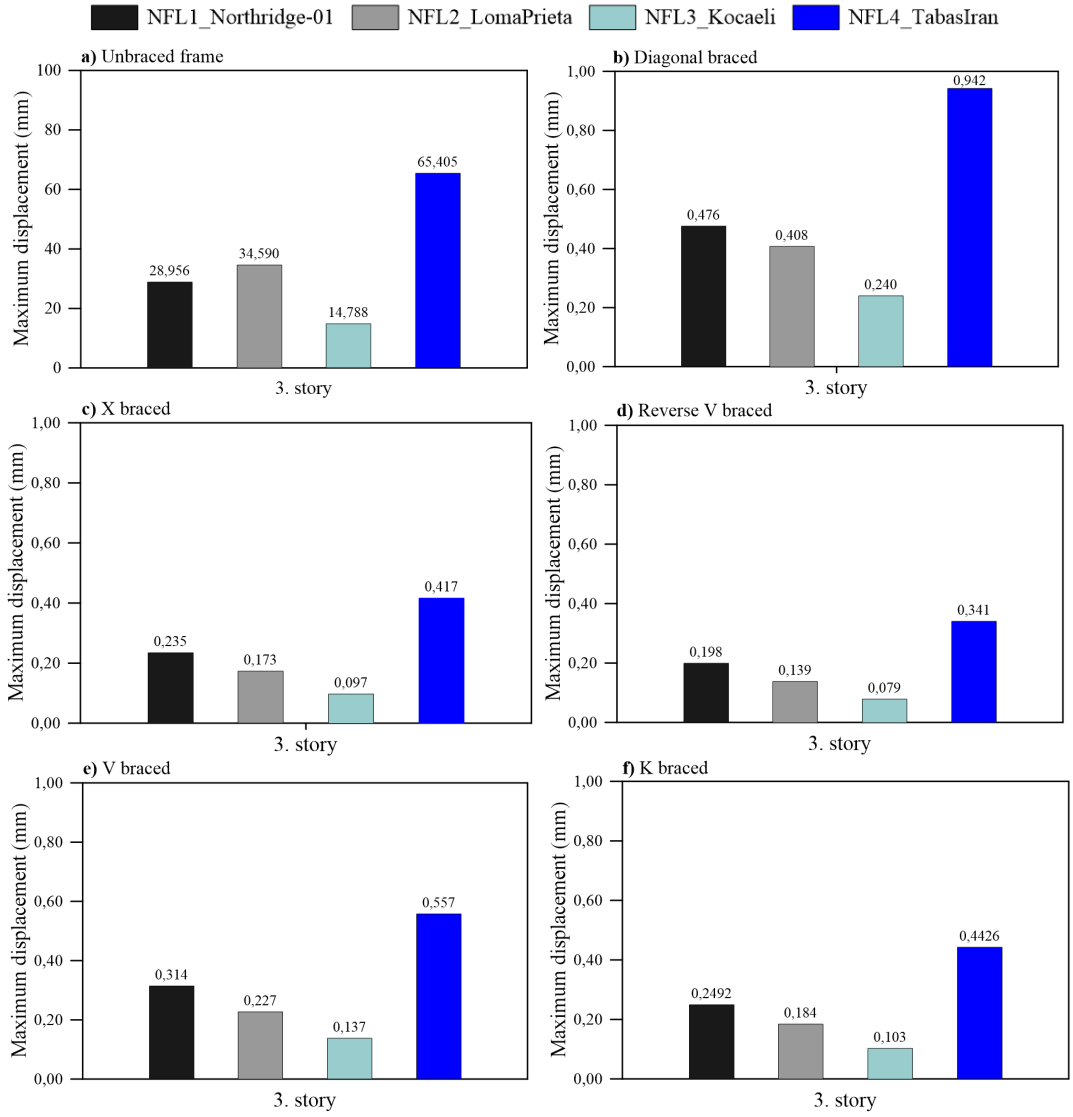

Figure 15. Maximum horizontal displacements considering different bracing models for the NFL.

The maximum top floor displacements under the NFL pulse motions are shown in Figure 15. The displacements for all frame systems are respectively obtained as 65.405 mm, 0.942 mm, 0.417 mm, 0.341 mm, 0.557 mm, and 0.443 mm under the Tabas-Iran earthquake, which has a large pulse and PGA value. Under the Loma-Prieta earthquake, which has a 3.98 s of pulse duration, the maximum top displacements are as 34.59 mm, 0.408 mm, 0.173 mm, 0.139 mm, 0.227 mm, and 0.184 mm for all frames, respectively. Likewise, the displacements are as 14.788 mm, 0.24 mm, 0.097 mm, 0.079 mm, 0.137 mm, and 0.103 mm under the Kocaeli-İzmit ground excitation, respectively. These ground excitations have nearly the same pulse duration and different PGA values. The displacement variation between the Tabas-Iran and Loma-Prieta earthquakes are 89%, 130%, 141%, 162%, 145%, and 141% for all frames, respectively. Moreover, the displacement variation between the Tabas-Iran and Kocaeli earthquakes is 343%, 290%, 329%, 331%, 306%, and 330% for all frames, respectively. In this manner, the low PGA values cause to lost efficiency according to the period of the structures but as long as PGA values are increased, the period effect has been very effective on structures for the NFL pulse motion.

In a general discussion, the triple displacement values for Loma-Prieta (NFL)-Northridge-01 (NFM)-Parkfield-02 (NFS) record motions are obtained as 34.59 mm-32.30 mm-41.70 mm, 0.408 mm-0.343 mm-0.366

mm, 0.173 mm-0.151 mm-0.182 mm, 0.139 mm-0.135 mm-0.151 mm, 0.227 mm-0.221 mm-0.233 mm and 0.184 mm-0.174 mm-0.193 mm for all frames, respectively. The double displacement values for Kobe-Japan (NFM) and Kobe-Japan (NFS) record motions are as 71.24 mm-87.64 mm, 0.65 mm-0.528 mm, 0.31 mm-0.30 mm, 0.26 mm-0.25 mm, 0.42 mm-0.38 mm, 0.33 mm-0.32 mm, for all frames, respectively. The double displacement values for Cape-Mendocino (NFM) and Kobe-Japan (NFS) record motions are as 40.50 mm-87.64 mm, 0.71 mm-0.528 mm, 0.33 mm-0.30 mm, 0.28 mm-0.25 mm, 0.43 mm-0.38 mm, 0.35 mm-0.32 mm, for all frames, respectively.

5. Conclusions and Recommendations

In the TBEC-2018, six different resisting frame systems have been suggested for steel structures such as moment resisting frame (unbraced frames), diagonally braced, X-braced, and reverse V-braced, V-braced, and K-braced. A comparison of the linear dynamic response characteristics of steel frame structures consisting of different resisting frame systems subjected to NF ground excitations which include pulse signals or have large velocity pulse duration is carried out in this study. For this purpose, a 3-story steel frame model composed of MRF and (CBFs) are analyzed using four different record motion sets, which are FF earthquakes, NF earthquakes with a small pulse (as an about 1 s), NF earthquakes with a medium pulse (as an about 2.80 s) and NF earthquakes with a large pulse (as an about 4 s). The investigation of the dynamic behavior of different steel resisting frames systems under pulse-like NF excitation has led to the following conclusions:

- The effects of PGA values on stiff systems are significant compared to flexible systems. Even though reverse V-braced systems, which have the lowest first mode period of vibration, occur minimum floor displacements under FF record motions, these systems are sensitive to PGA values. If the first mode period of vibration decreased, an increment in PGA values caused to larger structural demand. PGA could be identified as a key parameter that controls the response of braced frames under FF ground excitations.
- Although the diagonally braced frame systems have a larger first mode period of vibration according to other braced frames, these braced frames are not much affected under PGA for FF ground excitations.
- If NF ground excitations are taken into consideration as having a small pulse duration, which is only greater than the first mode period of bracing systems, it can be remarked that the ratio of T_p/T_1 is a dominant parameter even if PGA values are very large.
- Although the pulse duration, which is greater than the first mode period of vibration, is a dominant factor, but the rate of T_p/T_1 does not have a remarkable change on the structural demands as distinct from PGA values in consequence of the low first mode period of vibration.
- Although all braced systems have nearly same first mode period, especially diagonally braced and V-braced frame systems, which have a larger first mode period, are more sensitive to a pulse duration of ground excitations.

The results obtained from V-braced and reverse V-braced frame systems showed that the eccentricity can be more significant in eccentrically braced frames under pulse-like ground excitations. Future studies should examine the response of the pulse duration of ground excitations using nonlinear analysis of structures and fuse mechanisms instead of braces.

References

[1] Martinelli L, Mulas MG, Perotti F. The seismic response of concentrically braced moment-resisting steel frames. Earthquake Engineering & Structural Dynamics 1996; 25: 1275-1299.
[2] Balendra T, Huang X. Overstrength and ductility factors for steel frames designed according to BS 5950. Journal of Structural EngineeringJournal of Structural Engineering 2003;129: 1019-1035.
[3] Kim J, Choi H. Response modification factors of chevron-braced frames. Engineering Structures 2005; 27(2): 285-300.
[4] Dicleli M, Mehta A. Seismic performance of a special type of single-story eccentrically braced steel frame. Advances in Structural Engineering 2008; 11(1): 35-51.
[5] Khandelwal K, El-Tawil S, Sadek F. Progressive collapse analysis of seismically designed steel braced frames. Journal of Constructional Steel Research 2009; 65(3): 699-708.
[6] Coffield A, Adeli H. An investigation of the effectiveness of the framing systems in steel structures subjected to blast loading. Journal of Civil Engineering Management 2014; 20(6): 767-777.

[7] Shiravand MR, Shabani MJ. The effect of oblique blast loadings on moment and braced frames in steel structures. Advances in Structural Engineering 2016; 19(4): 563-580.
[8] Qi Y, Li W, Feng N. Seismic collapse probability of eccentrically braced steel frames. Steel and Composite Structures 2017; 24: 37-52.
[9] Larijan RJ, Nasserabadi HD, Aghayan I. Progressive collapse analysis of buildings with concentric and eccentric braced frames. Structural engineering and mechanics 2017; 61(6): 755-763.
[10] Bosco M, Marino E, Rossi P. A design procedure for dual eccentrically braced-moment resisting frames in the framework of Eurocode 8. Engineering structures 2017; 130: 198-215.
[11] Karsaz K, Tosee SVR. A comparative study on the behavior of steel moment-resisting frames with different bracing systems based on a response-based damage index. Civil Engineering Journal 2018; 4(6), 1354-1373.
[12] Yaman Z, Ağcakoca E. Performance Analysis of Circular Sieve Owner Center Steel Crosses. Sakarya University Journal of Science 2018; 22(2): 340-349.
[13] Faroughi A, Sarvghad Moghadam A, Ghanooni Bagha M. The Effects of Number and Location of Bracing Bays on Redundancy of Eccentrically-Braced Steel Moment Frames. Journal of Structural and Construction Engineering 2021; 8(8): 5-20.
[14] Altan Y. Merkezi ve dışmerkez çaprazlı çelik bina yapılarında deprem performansının belirlenmesi, Master thesis, İstanbul Gelişim Üniversity, Fen Bilimleri Enstitüsü, 2020.
[15] Yao Z, Wang W, Fang C, Zhang Z. An experimental study on eccentrically braced beam-through steel frames with replaceable shear links. Engineering Structures 2020; 206:110185.
[16] Haji M, Azarhomayun F, Ghiami Azad AR. Numerical investigation of truss-shaped braces in eccentrically braced steel frames. Magazine of Civil Engineering 2021; 2(102): 10208.
[17] Barbagallo F, Bosco M, Marino EM, Rossi PP. Seismic performance and cost comparative analysis of steel braced frames designed in the framework of EC8. Engineering Structures 2021; 240: 112379.
[18] Rouhi A, Hamidi H. Development of performance based plastic design of EBF steel structures subjected to forward directivity effect. International Journal of Steel Structures 2021; 21(3):1092-1107.
[19] Gürsoy Ş, Yılmaz A. Dış Merkezi Çelik Çapraz Tiplerinin Çerçeve Davranışına ve Yapı Maliyetine Etkisinin İncelenmesi. Düzce Üniversitesi Bilim ve Teknoloji Dergisi 2021; 9(5): 1766-1781.
[20] TBEC 2018. Turkish building earthquake code. Ministry of Environment and Urbanization of Turkey, Ankara, Turkey.
[21] Mahmoud S, Alqarni A, Saliba J, Ibrahim AH, Diab H. Influence of floor system on seismic behavior of RC buildings to forward directivity and fling-step in the near-fault region. Structures 2021; 30: 803-817.
[22] Somerville PG. Magnitude scaling of the near fault rupture directivity pulse. Physics of the earth and planetary interiors 2003; 137: 201-212.
[23] Yang D, Pan J, Li G. Interstory drift ratio of building structures subjected to near-fault ground motions based on generalized drift spectral analysis. Soil Dynamics and Earthquake Engineering 2010; 30(11): 1182-1197.
[24] Zou D, Han H, Liu J, Yang D, Kong X. 2017. Seismic failure analysis for a high concrete face rockfill dam subjected to near-fault pulse-like ground motions. Soil Dynamics and Earthquake Engineering 2017; 98: 235-243.
[25] Liao WI, Loh, CH, Lee, BH. Comparison of dynamic response of isolated and non-isolated continuous girder bridges subjected to near-fault ground motions. Engineering Structures 2004; 26(14): 2173-2183.
[26] Alavi B, Krawinkler H. Effects of near-fault ground motions on frame structures, John A. Blume Earthquake Engineering Center Stanford. 2001.
[27] Akkar S, Yazgan U, Gülkan P. Drift estimates in frame buildings subjected to near-fault ground motions. Journal of Structural Engineering 2005; 131(7):1014-1024.
[28] Malhotra PK. Response of buildings to near-field pulse-like ground motions. Earthquake Engineering and Structural Dynamics 1999; 28(11), 1309-1326.
[29] Chopra AK, Chintanapakdee C. Comparing response of SDF systems to near-fault and far-fault earthquake motions in the context of spectral regions. Earthquake engineering and structural dynamics 2001; 30(12): 1769-1789.
[30] Anderson JC, Bertero VV. Uncertainties in establishing design earthquakes. Journal of Structural Engineering 1987; 113(8): 1709-1724.
[31] Hayden C, Bray J, Abrahamson N, Acevedo-Cabrera A. Selection of near-fault pulse motions for use in design. 15th International World Conference on Earthquake Engineering; 2012; Lisboa.
[32] Alavi B, Krawinkler H. The behavior of moment-resisting frame structures subjected to near-fault ground motions. Earthquake engineering and structural dynamics 2004; 33(6): 687-706.
[33] Güneş N, Ulucan ZÇ. Nonlinear dynamic response of a tall building to near-fault pulse-like ground motions. Bulletin of Earthquake Engineering 2019; 17(6): 2989-3013.
[34] Seismosoft 2022. SeismoSignal-Signal Processing of Strong Motion Data.
[35] Kardoutsou V, Taflampas I, Psycharis. A new pulse indicator for the classification of ground motions. Bulletin of the Seismological Society of America 2017; 107(3): 1356-1364.
[36] PEER 2022. Ground motions Database Pacific Earthquake Engineering Research Center. University of California, California.
[37] ANSI, B. AISC 360-16, specification for structural steel buildings. Chicago AISC, 2016.
[38] Computers and Structures Inc. SAP2000: Static and Dynamic Finite Element Analysis of Structures, Berkeley, CA, U.S.A.